Contrast between 1992 and 1997 high latitude spring HALOE observations of lower stratospheric HCl

A. R. Douglass, S. R. Kawa

Atmospheric Chemistry and Dynamics Branch

NASA Goddard Space Flight Center

Greenbelt, MD

Short title:

Abstract. HCl measurements from HALOE in the northern hemisphere during mid-May 1997 revealed vortex fragments in which the chlorine reservoir partitioning was strongly pushed toward HCl ($\sim$90% HCl, $\sim$10% $ClONO_2$), similar to partitioning previously observed in the Antarctic vortex region. In contrast, observations of $ClONO_2$ and HCl in the northern polar spring, 1992, and in other years, show these species established the balance typical for gas phase photochemical reactions in this region ($\sim$60% HCl, $\sim$40% $ClONO_2$). Annually, chlorine reservoirs in the winter lower stratosphere polar vortex are converted to chlorine radicals via heterogeneous reactions on particle surfaces at very cold temperatures (less than about 200 K). As temperatures warm in spring, the heterogeneous processes become insignificant compared with gas phase reactions, and the chlorine reservoirs are reformed. Measurements through the northern winter/spring in 1992 show rapid formation of $ClONO_2$, followed by steady loss of $ClONO_2$ and increasing HCl. Although $ClONO_2$ measurements are not available for 1997, the HCl increase in 1997 is observed to be much more rapid and the eventual HCl mixing ratio is about 50% greater than that of 1992.

The observations are examined through comparison with the Goddard three-dimentsional chemistry and transport model. This model utilizes winds and temperatures from the Goddard Earth Observing System Data Assimilation System and a complete integration scheme for stratospheric photochemistry. Analysis of the evolution of HCl and $ClONO_2$ shows that the observed difference in the overall rate of HCl formation is explained by the sensitivity of the gas-phase chemistry to the ozone mixing ratio and the temperature. The results show that the model accurately simulates HCl and $ClONO_2$ evolution during these two winters. Model validity is further supported by comparisons with O_3 and reactive nitrogen species NO and NO_2. This analysis provides a sensitive test of the lower stratospheric chlorine photochemistry, particularly because the analysis considers constituent evolution at a time when the HCl and $ClONO_2$ are far from a photochemical stationary state.

1. Introduction

The northern hemisphere polar vortex was unusually cold and persistent during late winter and spring of 1997 [*Coy et al.*, 1997]. Ozone observed by the total ozone mapping spectrometer (TOMS) on the Advanced Earth Observing Satellite (ADEOS) was anomalously low [*Newman et al.*, 1997]. Temperatures were cold enough that heterogeneous reactions involving chlorine reservoir gases hydrochloric acid (HCl) and chlorine nitrate ($ClONO_2$) were expected to dominate the partitioning between chlorine reservoirs and radicals. In March 1997, low mixing ratios of HCl were observed at high latitudes by the Halogen Occultation Experiment (HALOE) on the Upper Atmosphere Research Satellite (UARS). The low HCl mixing ratios were inconsistent with gas phase photochemistry but consistent with heterogeneous chemical reactions which produce chlorine radicals Cl and ClO at the expense of the chlorine reservoirs HCl and $ClONO_2$ [*Müller et al.*, 1997]. Other articles describing the meteorology and constituent behavior for winter/spring 1997 are found in the November 1997 issue of *Geophysical Research Letters*.

Once the lower stratosphere warms and heterogeneous reactions cease to play a significant role in the partitioning among chlorine species, the chlorine radicals are converted to reservoirs via gas phase photochemical reactions. One pathway for removal of chlorine radicals is combination of ClO with the nitrogen radical NO_2. In the high latitude winter lower stratosphere, most nitrogen radicals are converted to nitric acid (HNO_3) by heterogeneous reactions, thus the formation of $ClONO_2$ follows release of NO_2 from HNO_3 by photolysis or reaction of HNO_3 with OH. In the northern lower stratosphere the increase of $ClONO_2$ is usually much more rapid than growth of HCl. Production of HCl takes place mainly through reaction of methane (CH_4) with atomic chlorine (Cl), whose concentration is small enough that this reaction is not favored, and the equilibrium between HCl and $ClONO_2$ is established slowly. Theoretical studies [e.g., *Prather and Jaffee*, 1990] and analysis of aircraft, ground based and satellite

observations from northern winters 1991-92 and 1992-93 support the paradigm of rapid loss of ClO and growth of $ClONO_2$ followed by a slow return to the balance between $ClONO_2$ and HCl appropriate for gas phase photochemical reactions [see *Santee et al.*, 1996a, and references therein].

The southern hemisphere winter vortex is significantly colder than its northern counterpart, and observations from aircraft and satellite indicate the permanent removal of HNO_3 from the stratosphere. In the absence of a source of nitrogen radicals, along with continued heterogeneous reactions, O_3 loss proceeds rapidly. Once O_3 falls below about 0.5 ppmv, the mixing ratio of Cl increases, and HCl formation is rapid. This was predicted by *Prather and Jaffee* [1990], and the rapid growth of HCl for very low O_3 was seen in HALOE HCl observations [*Douglass et al.*, 1995].

In spring 1997, mid-March HALOE observations at high latitudes showed HCl mixing ratios as low as 0.3 ppbv at 500K, indicative of ongoing or recent heterogeneous reactions. By mid May, some of the HCl mixing ratios observed by HALOE at 500 K were larger than 2 ppbv. Note that the lowest O_3 mixing ratios observed by HALOE in the vortex, about 1.5 ppmv, were much larger than those which accompany the rapid HCl formation seen in Antarctica, about 0.5 ppmv.

The Goddard three dimensional chemistry and transport model (CTM), initialized in mid-March 1997, produced an increase in lower stratospheric HCl that is consistent with these observations. The increase in the model took place over the course of a month. Inspection of the 6 northern springs observed by HALOE suggests that the HCl growth and high ratio to inferred Cl_y at 500K in 1997 is anomalous. The cause for the rapid 1997 increase in HCl is investigated here using comparisons of observations with the model fields, and calculations of constituent changes along parcel trajectories using the same chemical integration scheme as is used in the 3D model. Observations and the simulation are contrasted for the northern high latitude springs of 1997 and 1992.

There are several goals to this study. The first is to explain the observed behavior

of HCl, to identify the factors which control the rise in HCl once heterogeneous reactions directly involving HCl have ended, and to isolate the factors which are different in 1997 than in prior years. A second goal is to continue evaluation of the CTM. Direct comparisons of the model evolution with that observed for several constituents test the ability of the model to produce credible transport during the transition from the winter circulation, which is dominated by the polar vortex, to the summer circulation. In addition, such comparisons test the model photochemical scheme. In particular, these comparisons test the model representation of chlorine photochemistry when the chlorine reservoirs are undergoing rapid change driven by gas phase reactions, that is, when the reservoirs HCl and $ClONO_2$ are in the uncommon situation that their partitioning is far from a photochemical stationary state.

The data used in this study are described in the next section, followed by a description of the CTM in section 3. An overall comparison of model and observations is given in section 4. The model results for the reformation of the chlorine reservoirs are presented in section 5. This is followed by a discussion in section 6 and conclusions in section 7.

2 Data

The evolution of constituent fields from the CTM will be compared with observations from three of the instruments on the UARS satellite. A description of the UARS mission is given by *Reber et al.* [1993]. Each of the instruments of interest here is described briefly below.

2a Microwave Limb Sounder

The Microwave Limb Sounder (MLS) is described by *Barath et al.* [1993]. *Waters et al.* [1996] provide validation for ClO data obtained using the Version 3 algorithm. An improved algorithm has been used to reprocess MLS observations, and the reprocessed

version 4 data are used here. Briefly, there were two errors in the Version 3 ClO retrieval; an 8% scaling error and an additional high bias. The bias was produed when climatological HNO_3 greatly exceeded the atmospheric (gas phase) HNO_3; this is the case in the high latitude winter lower polar stratosphere when HNO_3 is often in a condensed phase [*Santee et al.*, 1996b]. MLS reports observations on alternate UARS standard pressure levels, including 100, 46, and 22 hPa. At 46 hPa, the pressure nearest the 500 K potentital temperature surface, the single profile 1-sigma precision is 0.5 ppbv; the estimated accuracy is 10%.

MLS provides temperature profiles which are coincident with the ClO profiles and are used for vertical interpolation of the MLS ClO mixing ratios to potential temperature surfaces. Although MLS measures temperature at 22 hPa and lower pressures; at higher pressures (the region of interest for this work), the temperatures are taken from the stratospheric analysis provided by the National Center for Environmental Prediction (NCEP), formerly the National Meteorological Center (NMC).

2b Cryogenic Limb Array Etalon Spectrometer

A description of the CLAES instrument is given by *Roche et al.* [1993]. The $ClONO_2$ profiles which are retrieved using algorithm version 7 are described by *Mergenthaler et al.* [1996]. The precision is within 15% between 50 and 10 hPa. The maximum systematic error is 28% between 100 and 10 hPa. Profiles retrieved using algorithm version 8 are used in this work. The version 7 data set encompasses January 9, 1992 - May 5, 1993. The version 8 data include this time period and also the earlier period October 21, 1991 to January 8, 1992. Data are reported on standard UARS pressure levels, which include 100, 68, 46 and 31 hPa, a separation of about 2.7 km. Comparisons of profiles shows very little difference between Version 7 and Version 8 $ClONO_2$ data sets for winter and spring 1992.

CLAES temperature profiles are used in the retrieval of the constituent mixing ratio

profiles as well as for vertical interpolation of the CLAES mixing ratios to potential temperature surfaces. The temperature validation is discussed by *Gille et al.* [1996].

2c Halogen Occultation Experiment

A description of the HALOE instrument is given by *Russell et al.* [1993]. HALOE observes vertical profiles using solar occultation. Approximately 15 sunrise and sunset measurements take place daily at each of two near constant latitudes. Profiles for the four constituents used here are retrieved using algorithm version 18. The vertical resolution of the HALOE observations is approximately 2 km. Validation of the HALOE ozone is discussed by *Brühl et al.* [1996]. The systematic plus random errors are shown to be about 18% at 40 hPa; the errors decrease at lower pressure but increase to 30% at 100 hPa. *Russell et al.* [1996] provide validation of HALOE HCl. The total error is estimated to be 12% at 5 hPa, and increases to 21% at 50 hPa. The HALOE NO and NO_2 measurements are described by *Gordley et al.* [1996]. There are significant errors in both NO and NO_2 below 25 km in spring 1992 due to Pinatubo aerosols. The aerosol loading has decreased greatly by the following spring and does not affect retrievals thereafter. In the lower stratosphere (below 25 km), HALOE NO_2 shows a low bias up to 0.5 ppbv. Between 25 and 40 km, agreement is within 10% of other observations. HALOE NO below 25 km, in the absence of volcanic aerosol, compares well with other observations when the concentration is large. Between 25 and 40 km, HALOE NO is consistently lower than correlative observations; the bias ranges from 0 to 15% at 25 km to 15 to 30% at 40 km.

HALOE provides temperature profiles coincident with constituent profiles which are used to interpolate the constituent mixing ratios to potential temperature surfaces. Temperatures are retrieved for levels above where aerosols affect the signals (35 km). Below this altitude, in the region of interest for this work, the temperature profiles are taken from NCEP.

3. Model Description

The CTM used here is an improved version of that used in previous analyses of observations from MLS, CLAES, and HALOE [*Kawa et al.*, 1995; *Douglass et al.*, 1997] and NIMBUS 7 TOMS observations [*Douglass et al.*, 1996]. Winds and temperatures used for 1992 simulations are taken from a stratospheric version of the Goddard Earth Observing System Data Assimilation System (GEOS DAS) described by *Schubert et al.* [1993]. The horizontal resolution of the assimilation fields in 1992 is 4° latitude by 5° longitude, and winds are interpolated to 2° latitude by 2.5° longitude for transport.

The assimilation system used to generate the meteorological fields for 1997 incorporates several important improvements. The system is described fully in the Algorithm Theoretical Basis Document of the Data Assimilation Office [*DAO*, 1997]. The improvements most relevant to the stratospheric analysis are summarized here. First, the computational pole is placed at the equator, thus the longitudinal grid spacing decreases as the Coriolis parameter decreases. This coordinate transformation reduces noise at high latitudes but has little impact on the tropical fields. Second, the top level of the general circulation model used in the assimilation has been raised to 0.1 hPa, compared with 0.4 hPa in the older system. This change and inclusion of a parameterization of gravity wave drag produce more realistic behavior at high latitudes, most notably increased descent within the polar vortex. The assimilation fields for 1997 are produced at 2° latitude by 2.5° longitude horizontal resolution.

The transport and photochemical contributions to the constituent continuity equation in the model are solved sequentially (process splitting). Advection is accomplished using the transport scheme developed by *Lin and Rood* [1996]. This scheme maintains sharp gradients and appropriate correlations for long-lived constituents, and does not produce unrealistic maxima or minima. For 1992, the assimilation winds are interpolated to the model vertical grid. For the 1997 integration, the winds are mapped onto the model vertical levels using an integration scheme developed by S. J.

Lin (personal communication). This mapping improves vertical transport in the mid to upper stratosphere, but has little impact on the lower stratosphere.

The photochemical scheme includes all gas phase reactions thought to be important in the stratosphere; rate constants are taken from *DeMore et al.* [1994]. Reactions on the surfaces of stratospheric aerosols are included, with aerosol surface area specified based on SAGE observations [*Thomason and Poole*, 1993] for 1992. For 1997 the surface area distribution for a volcanically clean atmosphere is taken from the *Scientific Assessment of Ozone Depletion: 1991* [*Albritton and Watson*, 1992]. This distribution agrees with aircraft measurements in the lower stratosphere to within 30%. Photolysis rates are calculated using temperature dependent cross sections [*DeMore et al.*, 1994] and reduced fluxes that are interpolated from a table-lookup based on the detailed radiative transfer calculations from the model of *Anderson and Lloyd* [1990]. The photolysis rates calculated in this way compare favorably with the photolysis benchmark which was developed as part of the AEAP program [*Stolarski et al.*, 1995]. This photochemical scheme is used in the CTM and also to calculate chemical evolution along trajectories; these calculations are initialized using 3D model fields.

For all simulations, the initialization for long lived species and families follows the procedure described by *Douglass et al.* [1997]. CLAES N_2O observations from mid November 1992 were mapped into a three dimensional grid using potential temperature as the vertical coordinate and potential vorticity for the horizontal structure. This field is mapped into an initial field, using the potential temperature and the potential vorticity fields for the desired day. Ozone is initialized using the same mapping procedure with MLS observations nearest to the initial day. For the remaining long-lived constituents and families, zonal average fields from the Goddard 2D model [*Jackman et al.*, 1996] are mapped onto the 3D grid using N_2O as the vertical coordinate. The NO_y initialization assumes that no widespread denitrification or dehydration has occurred in the vortex [*Santee et al.*, 1997]. The fields developed in this way show good agreement

with other observations; for example, the total ozone calculated from the initialization shows the same structure as TOMS observations.

The first day of the 1991-92 simulation is November 15, 1991. The simulation for 1997 was run in two parts. The first was initialized December 15, 1996, and run through March 31, 1997. This integration was made to compare the model ClO fields with MLS observations throughout the winter. The model was re-initialized March 18, 1997 and run through the northern 1998 spring and summer to be used in support of the Photochemistry of Ozone Loss in the Arctic Region in Summer (POLARIS) mission. The earlier integration agrees fairly well with the POLARIS integration during the period of overlap. The O_3 fields reveal the same horizontal structure, however, the vortex ozone from the Dec. 15, 1997 integration is high compared with observations, which impacts the partitioning among the chlorine species. This bias is likely at least partly due to a low model rate for O_3 destruction in the vortex, as reported recently by *Becker et al.,* [1998] and *Deniel et al.* [1998]. Because the O_3 must agree with observations to produce realistic growth and partitioning of chlorine species, this analysis will focus on the re-initialized POLARIS integration.

4. Overall Comparison of Model and Observations

This work focuses on the evolution of HCl in April and May for 1992 and 1997. For the model to be useful in this discussion, the model must accurately simulate the HALOE observations to the same degree for both integrations. Comparisons of HALOE observations of O_3, HCl, and sunset NO + NO_2 with model values of O_3, HCl, and NO_x= NO + NO_2 + $2N_2O_5$ are given in Plate 1. Model mixing ratios for the date and location of each HALOE observation are compared with the observed mixing ratios for pressure surfaces between 68 and 31 hPa for April 15-30 and July 11-13, 1992 and between 100 and 31 hPa for April 1-5 and June 6-12 1997. The 100 hPa level is not shown for 1992 because the HALOE observations are affected by the high concentration

of aerosols following eruption of Mt. Pinatubo. As noted in the validation paper, HALOE measurements of NO and NO_2 are accurate in the lower stratosphere when the aerosol loading is low and the mixing ratios of NO and NO_2 are high [*Gordley et al.,* 1996]. Only HALOE observations north of 50°N are considered.

The 1992 comparisons show that even after six months or more of integration, the model fields are in generally good agreement with the HALOE observations. In April, the model NO_X is up to 50% lower than the observations, which may indicate a problem in the model balance between the NO_X radicals and HNO_3 for high aerosol concentration, or too much aerosol input to the model. In July, when the sunlit period is longer and the importance of the heterogeneous reactions on sulfate aerosols is reduced, the comparison between the model NO_X and HALOE NO + NO_2 is improved though model NO_X is still low. In April, model O_3 is within 10% of HALOE observations. In July 1992 a high bias in O_3 ($\sim$ 12%) is evident at all three pressures. The model HCl is somewhat smaller than the HALOE HCl, in part due to the general problem that model total inorganic chlorine (Cl_y) in the lower stratosphere is about 20% less than the total Cl_y suggested by observations. Overall, these comparisons show that model fields are reasonably faithful to the observations for the nine months of integration.

The comparisons of model and observations for 1997 are also given in Plate 1. Although the model was initialized only a few weeks before, the model and observations are in good agreement for early April 1997. Comparisons for late March 1997 (not shown) are not as good, suggesting that the agreement between the model and data improves as the initialization adjusts to the GEOS DAS wind fields. The model NO_X agrees well with observations at the three highest pressures. At 31 hPa the model NO_X is up to 25% lower than the HALOE sunset NO + NO_2. Low model NO_X is also seen consistently in comparison to POLARIS ER-2 data (R. S. Gao, personal communication, 1998). The model is sampled without regard to local time, and the diurnal change in $ClONO_2$ is not accounted for, but this is not large enough to account

on the left. The model shows remnants of the polar vortex (high HCl, somewhat low O_3) near 60°N between 0°W and 90°W, between 60°E and 90°E, and near 30°N between 120°E and 180°E. The model also shows an area between 90°E and 120°E where tropical air which has low O_3 and low HCl has been transported poleward. HALOE observations on May 15 are near 60°N, spaced by about 24°, and should show large differences along the latitude circle. The model at 62°N is compared with the HALOE observations on the right side of Plate 2; model features in both HCl and O_3 compare well with HALOE observations. The good agreement and the higher than expected HCl mixing ratio observed by HALOE and produced by the model in the vortex fragments suggests the value of further analysis. This good agreement implies not only realistic photochemical changes, but also realistic breakup and transport of the polar vortex fragments, at least for the fragments sampled by HALOE.

5. Evolution of Chlorine Partitioning

In general, the evolution of chlorine species in the model matches that derived from observations for the time period when the chlorine reservoirs are being reformed and ClO and Cl_2O_2 are decreasing. This is illustrated for the 500K surface in Plate 3(a) for 1992 and Plate 3(b) for 1997. The labeled tick marks are the 15th of each month and unlabeled tick marks indicate the 1st of the month. The vortex average is calculated each day for model $ClO_x = ClO + 2Cl_2O_2$, HCl, $ClONO_2$ and Cl_y. The fractions ClO_x/Cl_y, $ClONO_2/Cl_y$, and HCl/Cl_y are given in the figure. Also shown on the plot are daily vortex sample averages for ratios of MLS daytime ClO, CLAES $ClONO_2$, and HALOE HCl to inferred vortex Cl_y. To plot these observations as fractions for comparison with model fractions, the vortex Cl_y is inferred from the average of the HCl, nighttime $ClONO_2$, and daytime ClO observations. The rationale is as follows. On February 12-17, 1992, the model vortex HCl is similar to the model average over the locations of the HALOE observations, which suggests that the HALOE average is

representative of the vortex. After UARS is yawed to view the northern hemisphere on February 14, the vortex average of model $ClONO_2$ is nearly equal to the average of the model at the locations of CLAES observations. The vortex average of model ClO_x is also approximated by the average of model ClO_x at the locations of MLS observations. Because of the consistency of the model vortex average with the average of model values as sampled by HALOE, MLS, and CLAES, we estimate the actual vortex average from the individual measurements in mid-February. Vortex average Cl_y is estimated to be 2.5 ppbv at 500 K based on these observations, compared with about 2 ppbv in the model.

Comparison of the constituent evolution with observations shows good consistency with the model evolution for 1992. Note that the measurement sampling may not be representative of the entire vortex, particularly for HALOE, and the model average at the location of the observations is also shown in Plate 3 for each constituent. When ClO is elevated early in winter, the evolution of MLS daytime ClO follows that of model ClO_x, the sum $ClO + 2\, Cl_2O_2$. Much of the difference between model ClO_x/Cl_y and MLS ClO/Cl_y is accounted for by inferring ClO_x from MLS ClO, assuming photochemical equilibrium between observed ClO and Cl_2O_2. Model $ClONO_2$ is about a factor of two smaller than CLAES data at this time. The reason for this difference is not clear. By early February however, the modeled evolution tracks the observations for all the Cl_y species. Vortex temperatures rose above the heterogeneous activation threshold ($\sim$ 195 K) on about January 30, 1992 [*Newman et al.*, 1993]. By middle February, CLAES and model show $ClONO_2/Cl_y \approx 0.6$. $ClONO_2$ peaks in early March, and ClO/Cl_y is small and nearly constant for the remainder of the integration. Model and HALOE indicate HCl/Cl_y is ≈ 0.25 in early February. The rate of HCl increase in the model accelerates once ClO/Cl_y reaches its minimum. The modeled and observed HCl/Cl_y are in good agreement in late March and early April, exhibiting similar growth. The vortex comparison ends when the vortex breaks apart and we cannot identify vortex fragments either in the observations or in the model.

Later in spring, the model and observations indicate little variance in HCl or nighttime $ClONO_2$ at 500K. The model averages on May 5 for the latitude band 40°N-50°N for HCl/Cl_y and $ClONO_2/Cl_y$ are indicated on Plate 3(a) by the large symbols. These are in good agreement with the fractions taken from averages of HALOE observations (about 42 °N) and CLAES nighttime ClONO2 in the same latitude band on May 5, also indicated by large symbols on the figure. This partitioning is similar to that reported by *Dessler et al.* [1995].

For 1997 there are many fewer observations for comparison. There are no measurements of $ClONO_2$ during 1997. The vortex average Cl_y is estimated from the mid-May HALOE HCl observations and the model $ClONO_2/HCl$, and compares well with Cl_y inferred from HALOE CH_4 [*Dessler et al.*, 1997]. The vortex average model ClO_x/Cl_y increases to a maximum of about 0.8 in late January. There is a broad peak of about 0.6 throughout February, and a rapid decline in early March. The average of the MLS ClO/Cl_y agree fairly well with the model ClO_x/Cl_y at the location of the MLS observations. $ClONO_2/Cl_y$ again peaks at about 0.8, as in 1992, but the maximum occurs several weeks later. HCl/Cl_y rises from about 0.2 in early March to greater than 0.5 by about March 20; both modeled and observed HCl/Cl_y continue to increase. This rise during early March is steeper than is seen in 1992, when modeled HCl/Cl_y is about 0.25 on March 1 and reaches 0.35 by about March 20. The low fraction for HCl/Cl_y on March 1 is consistent with the later occurrence in 1997 of temperatures cold enough that heterogeneous reactions which reduce the chlorine reservoirs dominate the chlorine partitioning. The area of temperatures cold enough for rapid heterogeneous chlorine activation declined sharply in late February, 1997 [*Santee et al.*, 1997]. Intermittent small areas of temperature below 195 K, however, persisted through March, which explains the relatively higher ClO amounts. In mid March 1997, model HCl/Cl_y is in fair agreement with HALOE HCl/Cl_y and the model partitioning between HCl and ClONO2 is slightly shifted towards HCl compared to the partitioning inferred for 1992.

Throughout April 1997, unlike April 1992, the model HCl continues to increase rapidly. The increase is confirmed by HALOE HCl, which shows a change between late March and middle May that is nearly identical to the modeled change. Note that this good agreement implies realistic breakup and transport of the polar vortex fragments, at least for the fragments sampled by HALOE.

In summary, the comparison between 1992 and 1997 shows that colder temperatures and a more enduring vortex lead to a later recovery of reactive ClO_x to HCl and $ClONO_2$ in 1997. In addition, the recovery pathway in 1997 produces much more HCl than $ClONO_2$ and the the ultimate $HCl/ClONO_2$ in 1997 greatly exceeds that in 1992. We will show that the difference in recovery pathways is primarily the result of lower O_3 in 1997 along with lower temperature. The 1997 case is similar to that for the Antarctic collar during spring of 1992 [*Douglass et al.*, 1995]. Note that in spite of the differences in chlorine partitioning there does not appear to be a feedback on O_3, at least for these specific cases. The chlorine-induced O_3 loss for the two cases is nearly the same after March 20, consistent with the low ClO_x.

To account for the springtime differences in the HCl evolution in 1992 and 1997, forward trajectories were calculated for March 28 - April 19 for both 1992 and 1997. The initial points for the trajectories are the locations of high latitude HALOE observations on March 28. The photochemical evolution along these trajectories was calculated, initialized from the 3D model fields, and noting general consistency between the initialization from the model and the HALOE observations.

For 1992, all parcels show the same behavior for HCl (Figure 1a). The tendency in HCl is small - the maximum change in HCl over the 20 day period is less than 0.2 ppbv. In 1997, parcels fall into two categories (Figure 1b). For parcels in the first category, the HCl mixing ratio is nearly steady, and is similar to the HCl mixing ratio in the 1992 parcels. For parcels in the second category, HCl increases by up to 0.55 ppbv over 20 day integration. On average, the HCl mixing ratio at the end of this integration for parcels

in the second category is 0.5 ppbv higher than that for the first category parcels. The potential vorticity calculated from the assimilation wind fields is on average 60% higher for the trajectories of the parcels in which the HCl increases, evidence that these parcels were part of the polar vortex. At the end of the integration, the results of the trajectory calculation for constituents including HCl, $ClONO_2$, and O_3 compare well with the model fields at the model location nearest the trajectory endpoint. This is illustrated by Figure 1(c), which shows the difference in initial and final HCl calculated using the trajectory model and calculated using the 3D model field at the model location nearest the initial and final points of the trajectories. This good agreement supports the use of the trajectory model for analysis of the processes contributing to the growth in HCl and leading to a final HCl/Cl_y in ex-vortex air which is much greater than in surrounding air.

6. Discussion

The principle gas phase production and loss processes for HCl in the lower stratosphere are

$$Cl + CH_4 \rightarrow HCl + CH_3 \tag{1}$$

$$HCl + OH \rightarrow Cl + H_2O \tag{2}$$

Other production processes such as the reaction of ClO with OH and reaction of Cl with H_2, H_2O_2, and HO_2 and other loss processes such as photolysis of HCl are included in the model but play a minor role in the HCl evolution and are not considered in the following discussion. Heterogeneous reactions which take place on aerosols, HCl + $ClONO_2$ and HCl + HOCl, are also included in the model but are not significant for

these trajectories compared to gas phase reactions.

Neglecting transport and mixing, the continuity equation for the HCl mixing ratio X_{HCl} is written

$$\frac{dX_{HCl}}{dt} = K_{Cl,CH4}[Cl]X_{CH4} - K_{HCl,OH}[OH]X_{HCl} \tag{3}$$

where X_{CH4} is the methane mixing ratio. The 48 hour average production and loss for all parcels are compared in Figure 2. The maximum and minimum of the average production and loss for all 1992 parcels are shown by the shaded bands. The daily maximum average values for each of the 1997 parcels are given individually. Production for all parcels in 1992 is about 0.02 ppbv/day. For some of the parcels in 1997 (solid lines in Figures 1(b) and 2), production is in a similar range. For the parcels in which HCl is increasing, production is larger, up to an average of about 0.05 ppbv/day. The loss is similar in both years for most of the integration (Figure 2b). HCl is somewhat higher in 1997 (Figure 1), but OH is somewhat higher in 1992. (The increase in modeled OH is due to Mt. Pinatubo aerosols, which speed the reactions $H_2O + N_2O_5 \rightarrow 2$ HNO_3 and $H_2O + BrONO_2 \rightarrow HNO_3 + HOBr$; photolysis of HNO_3 and HOBr leads to higher production of hydrogen radicals.) For all 1992 parcels and some 1997 parcels, the loss is approximately equal to production. For parcels with increasing HCl, the loss (which is proportional to HCl) increases throughout the integration, and is approaching balance with the production at the end of the integration. This is in general agreement with Plate 3. In 1992, HCl is nearly constant by April 1. In 1997, the HCl levels off during mid to late April. When HALOE samples the high HCl air in mid-May as in Plate 2, the HCl is in approximate photochemical balance.

It is obvious from Figure 2 that the large difference in production is responsible for the observed difference in HCl evolution. Since X_{CH4} is comparable in the model in 1992 and 1997, the product of the mixing ratio of Cl and the reaction rate $K_{Cl,CH4}$

must be greater for the parcels in which HCl is increasing. Model output shows that the rate $K_{Cl,CH4}$ is larger (due to the lower temperature) and the mixing ratio of Cl is also larger. Insight is gained by considering the factors which produce this difference in the production of chlorine reservoirs. The production in parts per second can be written

$$P_{HCl} = K_{CH4,Cl} X_{CH4} \times \frac{[Cl]}{[ClO]} \times \frac{[ClO]}{[ClONO_2]} \times [ClONO_2] \tag{4}$$

The fractions Cl/ClO and ClO/ClONO$_2$ are replaced in (4) by relationships which are derived from principle production and loss processes:

$$\frac{[Cl]}{[ClO]} = \frac{K_{ClO,O}[O] + K_{ClO,NO}[NO]}{K_{Cl,O3}[O_3]} \tag{5}$$

$$\frac{[ClO]}{[ClONO_2]} = \frac{J_{ClONO2}}{K_{ClO,NO2,M}[NO_2][M]} \tag{6}$$

Neglecting $K_{ClO,O}[O]$ compared with $K_{ClO,NO}[NO]$ in the numerator of (5), substituting (5) and (6) into (4) and regrouping yields

$$P_{HCl} = K_{CH4,Cl} X_{CH4} \times \frac{K_{ClO,NO}}{K_{Cl,O3}[O_3]} \times \frac{J_{ClONO2}}{K_{ClO,NO2,M}} \times \frac{[NO]}{[NO_2]} \times X_{ClONO2} \tag{7}$$

The nitrogen radicals are related through principle production and loss processes

$$\frac{[NO]}{[NO_2]} = \frac{J_{NO2}}{K_{NO,ClO}[ClO] + K_{NO,O3}[O_3]} \tag{8}$$

Substituting for NO/NO$_2$ from (8) into (7) yields

$$P_{HCl} = K_{CH4,Cl}X_{CH4} \times \frac{K_{ClO,NO}}{K_{Cl,O3}[O_3]} \times \frac{J_{ClONO2}}{K_{ClO,NO2,M}}$$
$$\times \frac{J_{NO2}}{K_{NO,ClO}[ClO] + K_{NO,O3}[O_3]} \times X_{ClONO2} \qquad (9)$$

The term $K_{NO,ClO}[ClO]$ dominates the denominator of (8) when ClO is elevated. For example, for $O_3 \sim 2.4$ ppmv, and the temperature between 200 and 210 K, $K_{NO,ClO}[ClO]$ is larger than $K_{NO,O3}[O_3]$ when $[ClO] \geq 0.3$ ppbv. Photolysis of HNO_3 and reaction of HNO_3 with OH produces nitrogen radicals, and $ClONO_2$ growth must precede growth of HCl.

ClO decreases steadily as NO_X is produced and $ClONO_2$ increases, and the reaction of NO with ClO becomes less important than the reaction of NO with O_3 in controlling the ratio NO/NO_2. The reaction of NO with O_3 becomes dominant once the mixing ratio of NO_X is of the same order as the mixing ratio of ClO_X. There is aerosol dependence implicit in this condition - higher aerosol loading is consistent with lower mixing ratio for NO_X (Plates 1 and 2) and higher ClO [*Fahey et al.*, 1993]. The growth rate of HCl in 1992 increases when ClO/Cl_y has fallen to about 0.1. At this point in the model, the mixing ratio of ClO_X is approximately equal to the mixing ratio of NO_X.

Once the ClO mixing ratio has decreased through formation of $ClONO_2$ so that $NO + O_3$ is the more important term in controlling the ratio NO/NO_2, the production for a parcel on a constant potential temperature surface may be approximated

$$P = K_{CH4,Cl}X_{CH4} \times \frac{K_{ClO,NO}}{K_{Cl,O3}X_{O3}[M]} \times \frac{J_{ClONO2}}{K_{ClO,NO2,M}} \times \frac{J_{NO2}}{K_{NO,O3}X_{O3}[M]} \times X_{ClONO2} \qquad (10)$$

This expression depends on the photolysis rates, the methane mixing ratio, the inverse square of the ozone mixing ratio, and the temperature through the kinetic rates and through the density. It applies to both cases after about March 15. The photolysis

rates for $ClONO_2$ and NO_2 are nearly equal during 1992 and 1997. The methane mixing ratio is also nearly constant. As noted in the Introduction, the polar vortex in 1997 is cold and long lasting, and the temperature difference between 1992 parcels and the 1997 parcels in which HCl grows is about 15K. The ozone mixing ratio difference for these same parcels is about 20%, i.e., the ozone mixing ratio is 0.4-0.6 ppmv lower in parcels in which the HCl grows. The production is also a function of the mixing ratio of $ClONO_2$ which is near constant for 1992 but is decreasing throughout the integration for 1997 (see Plate 3(b)). As the mixing ratio of $ClONO_2$ decreases, the production and loss come into balance, and the HCl mixing ratio becomes constant (see Plate 3(a)).

Equation 10 provides a simple means to evaluate the relative importance of the factors which contribute to a difference in production, i.e., the O_3 mixing ratio, the temperature, the CH_4 mixing ratio, and $ClONO_2$ mixing ratio, and the photolysis rates. The factors which themselves have the largest fractional changes are the O_3 mixing ratio and the temperature. The fractional changes in the CH_4 mixing ratio and the photolysis rates are small compared to those of the ozone mixing ratio and the temperature. Neglecting these smaller contributions, combining the temperature dependences for all of the reaction rates, using the low pressure limit for the association reaction of ClO and NO_2, and noting that $\Delta M/M = 2.5\Delta T/T$ on a constant potential temperature surface, the expected fractional difference in HCl production, i.e., $\Delta P/\overline{P} = (P_{1997} - P_{1992})/(P_{1997} + P_{1992}) \times 2$, is given by

$$\frac{\Delta P}{\overline{P}} = \frac{-2\Delta O_3}{\overline{O_3}} - \left(\frac{550}{\overline{T}} + 1.6\right)\frac{\Delta T}{\overline{T}} \tag{11}$$

Here, ΔO_3 is the difference in O_3 and ΔT is the difference in temperature between two parcels (1997-1992), and the overbar indicates the average. In Figure 3 we show that the expression of the right hand side of (11) is a good approximation for the fractional difference in the production for two parcels when the production for each parcel is calculated from (10). We compare a parcel from 1997 in which HCl is increasing with a

parcel from 1992. For the time period shown, $\Delta P/\overline{P}$ calculated from (11) and $\Delta P/\overline{P}$, calculated using the production of each parcel evaluated using (10), differ by less than 5%. At $\Delta P/\overline{P} = 0.67$, the production rate for 1997 is twice that of 1992. The low ozone is the most important cause of the more rapid increase in HCl in 1997 and the higher HCl in steady state. The effect of the temperature difference is far from negligible; on average the temperature difference is responsible for 30% of the difference in production rate. The high HCl disappears after the low vortex O_3 dissipates completely in late May.

7. Conclusions

The unusually cold stable polar vortex and the low O_3 observed in spring 1997 led to an observable difference in the reformation of chlorine reservoirs in 1997 compared with 1992. The northern vortex was more like the southern winter vortex in that it lasted well into spring, but the observed O_3 was not as low as is observed in the Antarctic. Nonetheless, relatively low O_3 and cold temperatures combine to give a faster increase in HCl, and the steady state partitioning between HCl and $ClONO_2$ is pushed towards HCl, resembling the partitioning seen in the Antarctic. The 3D model calculations are in good overall agreement with the HALOE observations.

The breakup of the polar vortex, the transport of fragments, and the photochemical change within the vortex fragments produced by the CTM are in overall good agreement with the observations available for this time period. There have been other examples of lower stratospheric transport on similar temporal and spatial scales which point to the applicability of transport calculated with assimilation winds. These comparisons are unique in that the photochemical changes produced in HCl and $ClONO_2$ are substantial throughout the periods of comparison. Furthermore, the model allows interpretation of the difference in the growth rate of HCl in terms of other observed quantities, O_3 and temperature. These comparisons show that the model captures the essential components of chlorine photochemistry for an evolving system, a much stronger test than obtained

by comparing partitioning for constituents near steady state.

This work expands the view of reformation of chlorine species. In 1992 and 1993, the years for which the CLAES instrument observed $ClONO_2$ in the northern spring vortex, the O_3 mixing ratio was significantly larger than in 1997. The balance between HCl and $ClONO_2$ was established slowly; the fraction HCl/Cl_y exceeded the fraction $ClONO_2/Cl_y$ by about 0.2 at steady state. This contrasts with 1997, when low O_3 and cold temperatures combine to produce a balance between the chlorine reservoirs within the persistent polar vortex which is pushed strongly towards HCl. In 1997, (observed) $HCl/Cl_y \sim 0.8$-0.9, implying that $ClONO_2/Cl_y \sim 0.2$-0.1. This work emphasizes that the rate of HCl production and the balance between chlorine reservoirs established following the cessation of heterogeneous reactions on PSCs is a sensitive function of O_3 and temperature.

References

Albritton, D. L., and R. T. Watson, Co-Chairs, Scientific Assessment of Ozone Depletion: 1991, *World Meteorological Organization Global Ozone Research and Monitoring Project - Report No. 25*, 1992.

Anderson, D. E., Jr., and S. A. Lloyd, Polar twilight UV-visible radiation field: perturbations due to multiple scattering, ozone depletion, stratospheric clouds, and surface albedo, *J. Geophys. Res., 95*, 7429-7434, 1990.

Barath, F., et al., The upper atmosphere research satellite microwave limb sounder instrument, *J. Geophys. Res., 98*, 10751-10762, 1993.

Becker, G., R. Müller, D. McKenna, and M. Rex, Modeled ozone loss rates in the arctic stratosphere compared with results of the Match experiments, *EOS Trans. AGU, 79(17)*, Spring Meeting Suppl., S30, 1998.

Brühl, C. et al., Halogen Occultation Experiment ozone channel validation, *J. Geophys. Res., 101*, 10,217-10,240, 1996.

Coy, L., E. R. Nash, and P. A. Newman, Meteorology of the polar vortex: spring 1997, *Geophys. Res. Lett., 24*, 2693-2696, 1997.

DAO, Algorithm Theoretical Basis Document Version 1.01, Data Assimilation Office, NASA Goddard Space Flight Center, 1996.

DeMore, W. B., et al., Chemical kinetics and photochemical data for use in stratospheric modeling, *JPL Publication 94-20*, NASA, 1994.

Deniel, C., R. Bevilacqua, F. Lefèvre, J. Pommereau, *EOS Trans. AGU, 79(17)*, Spring Meeting Suppl., S30, 1998.

Dessler, A. E., D. B. Considine, G. A. Morris, M. R. Schoeberl, A. E. Roche, J. M. Russell, J. W. Waters, J. B. Kumer, J. L. Mergenthaler, J. C. Gille, and G. K. Yue, Correlated observations of HCl and $ClONO_2$ from UARS and implications for stratospheric chlorine partitioning, *Geophys. Res. Lett., 22*, 1721-1724, 1995.

Dessler, A. E., D. B. Considine, J. E. Rosenfield, S. R. Kawa, A. R. Douglass, and J. M. Russell, III, Lower stratospheric chlorine partitioning during the decay of the Mt. Pinatubo cloud, *Geophys. Res. Lett., 24*, 1623-1626, 1997.

Douglass, A. R., M. R. Schoeberl, R. S. Stolarski, J. W. Waters, J. M. Russell III, A. E. Roche, S. T. Massie, Interhemispheric differences in springtime production of HCl and ClONO$_2$ in the polar vortices, *J. Geophys. Res., 100*, 13,967-13,978, 1995.

Douglass, A. R., C. J. Weaver, R. B. Rood and L. Coy, A three dimensional simulation of the ozone annual cycle using winds from a data assimilation system, *J. Geophys. Res., 101*, 1463-1474, 1996.

Douglass, A. R., R. B. Rood, S. R. Kawa, and D. J. Allen, A three dimensional simulation of the middle latitude winter ozone in the middle stratosphere, *J. Geophys. Res., 102*, 19,217-19,232, 1997.

Fahey, D. W., et al., In situ measurements constraining the role of sulphate aerosols in mid-latitude ozone depletion, *Nature, 363*, 509-514, 1993.

Gille, J. C., et al., Accuracy and precision of cryogenic limb array etalon spectrometer (CLAES) temperature retrievals, *J. Geophys. Res., 101*, 9583-9601, 1996.

Gordley, L. L., et al., Validation of nitric oxide and nitrogen dioxide measurements made by the Halogen Occultation Experiment for UARS Platform, *J. Geophys. Res., 101*, 10,241 - 10,266, 1996.

Jackman, C. H., E. L. Fleming, S. Chandra, D. B. Considine, J. E. Rosenfield, Past present and future modeled ozone trends with comparisons to observed trends, *J. Geophys. Res., 101*, 28,753-28,767, 1996.

Kawa, S. R., J. B. Kumer, A. R. Douglass, A. E. Roche, S. E. Smith, F. W. Taylor, and D. J. Allen, Missing chemistry of reactive nitrogen in the upper stratospheric polar winter, *Geophys. Res. Lett., 22*, 2629-2632, 1995.

Lin, S. J., and R. B. Rood, Multidimensional flux form semi-Lagrangian transport schemes, *Mon. Wea. Rev., 124*, 2046-2070, 1996.

Mergenthaler, J. L., et al., Validation of CLAES ClONO$_2$ measurements, *J. Geophys. Res.,* *101,* 9,603-9,621, 1996.

Müller, R., J.-U. Grooß, D. S. McKenna, P. J. Crutzen, C. Brühl, J. M. Russell III, A. F. Tuck, HALOE observations of the vertical structure of chemical ozone depletion in the Arctic vortex during winter and early spring 1996-1997, *Geophys. Res. Lett., 24,* 2717-2720, 1997.

Newman, P. A., et al., Stratospheric meteorological conditions in the Arctic polar vortex, 1991 to 1992, *Science, 261,* 1143-1146, 1993.

Newman, P.A., J. F. Gleason, R. D. McPeters, and R. S. Stolarski, Anomalously low ozone over the Arctic, *Geophys. Res. Lett., 24,* 2689-2692, 1997.

Prather, M. P. and A. H. Jaffe, Global impact of the antarctic ozone hole: chemical propagation, *J. Geophys. Res., 95,* 3473-3492, 1990.

Reber, C. A., C. E. Trevathan, R. J. McNeal, and M. R. Luther, The Upper Atmosphere Research Satellite (UARS) mission,*J. Geophys. Res., 98,*10,643-10,647, 1993.

Roche, A. E., J. B. Kumer, J. L. Mergenthaler, G. A. Ely, W. G. Uplinger, J. F. Potter, T. C. James, and L. W. Sterritt, The cryogenic limb array etalon spectrometer (CLAES) on UARS: Experiment description and performance, *J. Geophys. Res., 98,* 10,763-10,775, 1993.

Russell, J. M. III, L. L. Gordley, J. H. Park, S. R. Drayson, A. F. Tuck, J. E. Harries, R. J. Cicerone, P. J. Crutzen and J. E. Frederick, The Halogen Occultation Experiment, *J. Geophys. Res., 98,* 10,777-10,797, 1993.

Russell, J. M. III, et al., Validation of hydrogen chloride measurements made by the Halogen Occultation Experiment from the UARS platform, *J. Geophys. Res., 101,* 10,151-10,162, 1996.

Santee, M., L. Froidevaux, G. Manney, W. Read, J. Waters, M. Chipperfield, A. Roche, J. Kumer, J. Mergenthaler, and J. Russell III, Chlorine deactivation in the lower

stratospheric polar regions during late winter: Results from UARS *J. Geophys. Res.,* *101,* 18,835-18,859, 1996a.

Santee, M., G. Manney, W. Read, L. Froidevaux and J. Waters, Polar vortex conditions during the 1995-96 Arctic winter: MLS ClO and HNO_3, *Geophys. Res. Lett., 23,* 3207-3210, 1996b.

Santee, M. L., G. L. Manney, L. Froideveaux, R. W. Zurek, and J. W. Waters, MLS observations of ClO and HNO3 in the 1996-1997 Arctic polar vortex, *Geophys. Res. Lett., 24,* 2713-2716, 1997.

Schubert, S., R. Rood, J. Pfaendtner, An assimilated dataset for earth science applications, *Bull. Amer. Soc., 74,* 2331-2342, 1993.

Stolarski, R. S. and others, 1995 Scientific Assessment of the Atmospheric Effects of Stratospheric Aircraft, NASA Reference Publication 1381, 1995.

Thomason, L. J., and L. R. Poole, Use of stratospheric aerosol properties as diagnostics of Antarctic vortex processes, *J. Geophys. Res., 98,* 23,003-23,012, 1993.

Waters, J. W., W. G. Read, T. A. Lungu, L. Froidevaux, V. S. Perun, R. A. Stachnik, R. F. Jarnot, R. E. Cofield, E. F. Fishbein, D. A. Flower, J. R. Burke, J. C. Hardy, L. L. Nakamura, B. P. Ridenoure, Z. Shippony, R. P. Thurstans, L. M. Avallone, D. W. Toohey, R. L. deZafra, and D. T. Shindell, Validation of UARS MLS ClO measurements, *J. Geophys. Res., 101,* 10091-10127, 1996.

Figure 1. (a) In 1992, the HCl mixing ratio is constant on all trajectories; (b) In 1997, the HCl mixing ratio is constant on one group of the trajectories (solid lines), but increases rapidly for the second group (dashed lines); (c) the difference HCl_f- HCl_i calculated from the 3D model values nearest the initial and final points of the trajectory (x axis) agrees well with the difference calcualted from the trajectory model (y axis), supporting the use of the trajectory model in this analysis.
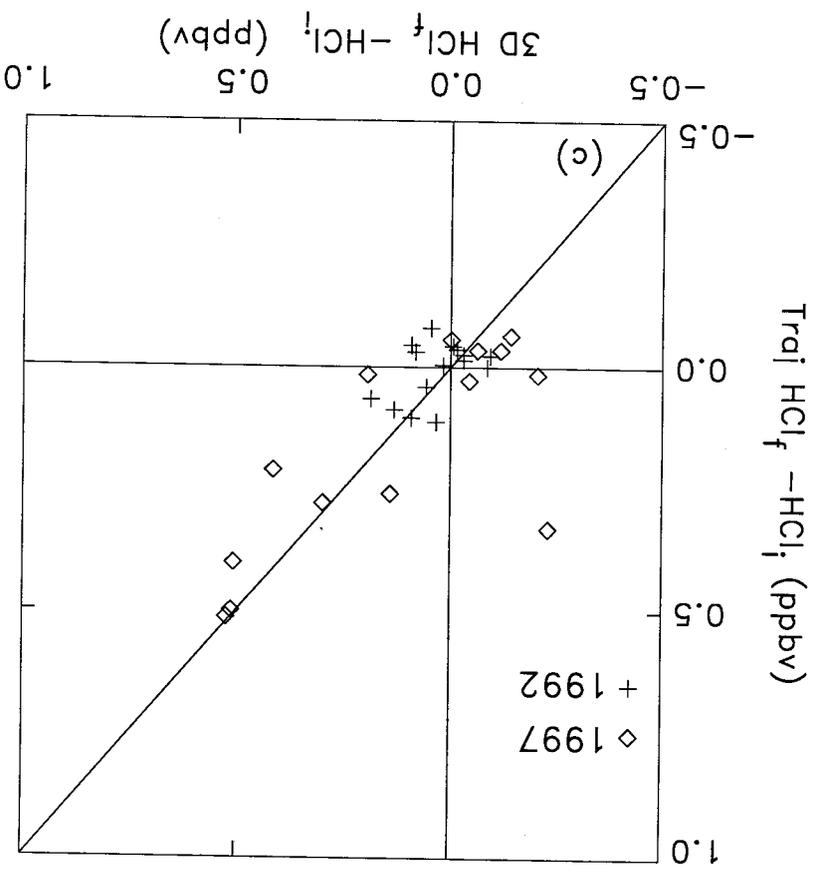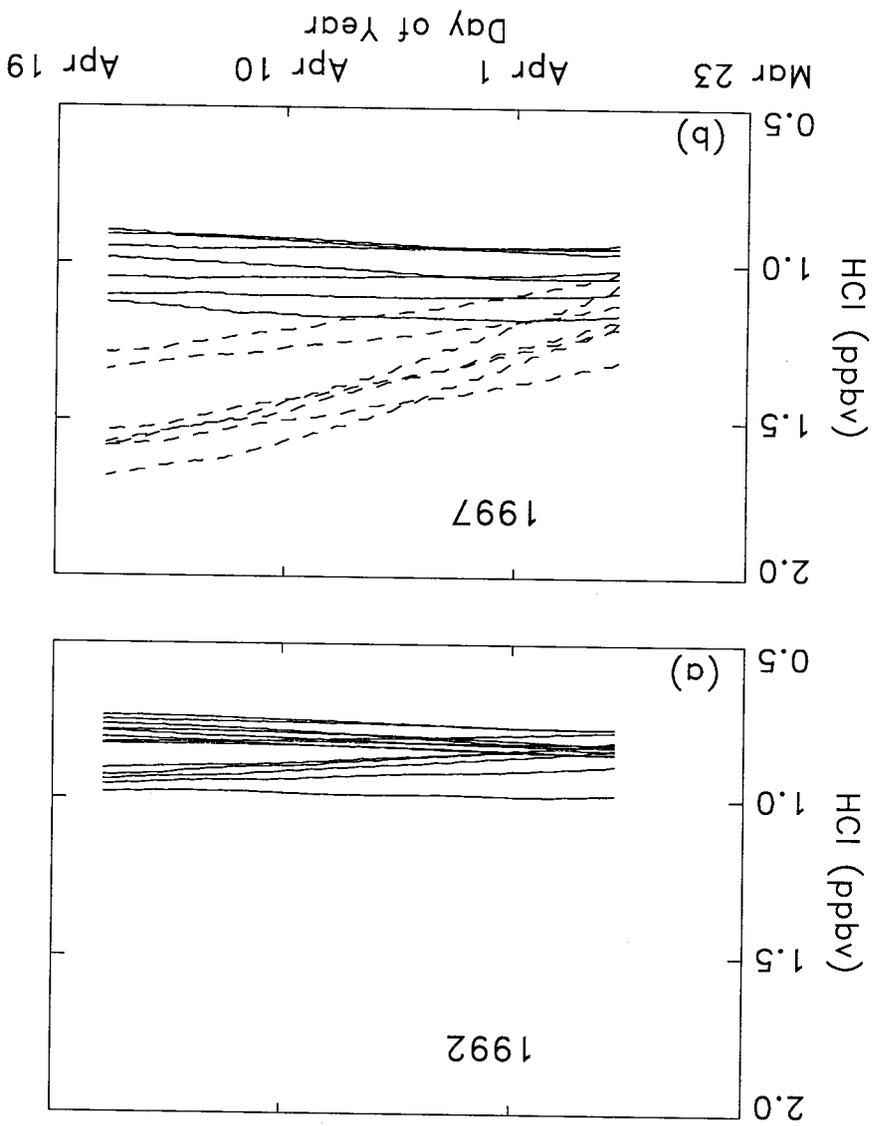
Figure 2. (a) The 48 hour average production calculated for some 1997 parcels in Figure 1(b) (solid lines) is comparable to the production for the 1992 parcels in Figure 1(a)(shaded area), but is much larger for other 1997 parcels (dashed lines). (b) The loss is similar for both groups of 1997 parcels, until towards the end of the integration when the loss (which is proportional to HCl) increases for the parcels which have experienced the growth in HCl.

Figure 3. The fractional difference in production ($\Delta P/\overline{P} = (P_{1997} - P_{1992})/(P_{1997} + P_{1992}) \times 2$ where P_{1997} and P_{1992} are calculated from (10), and the contributions to that difference from O_3 and temperature as given by (11)

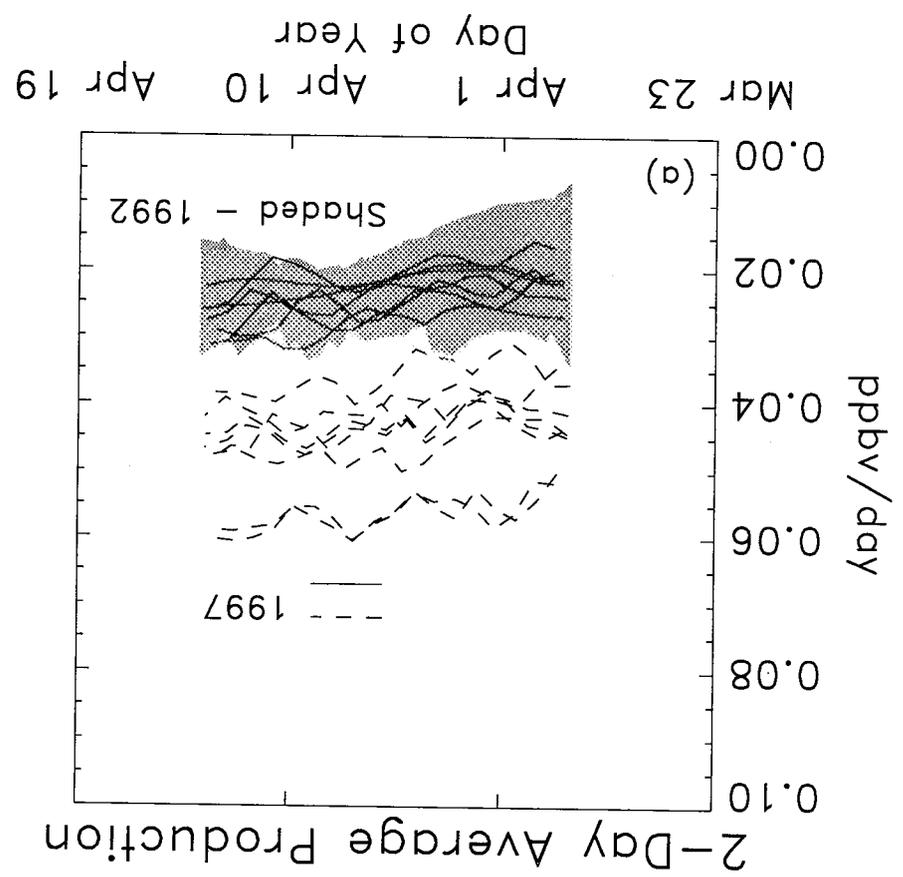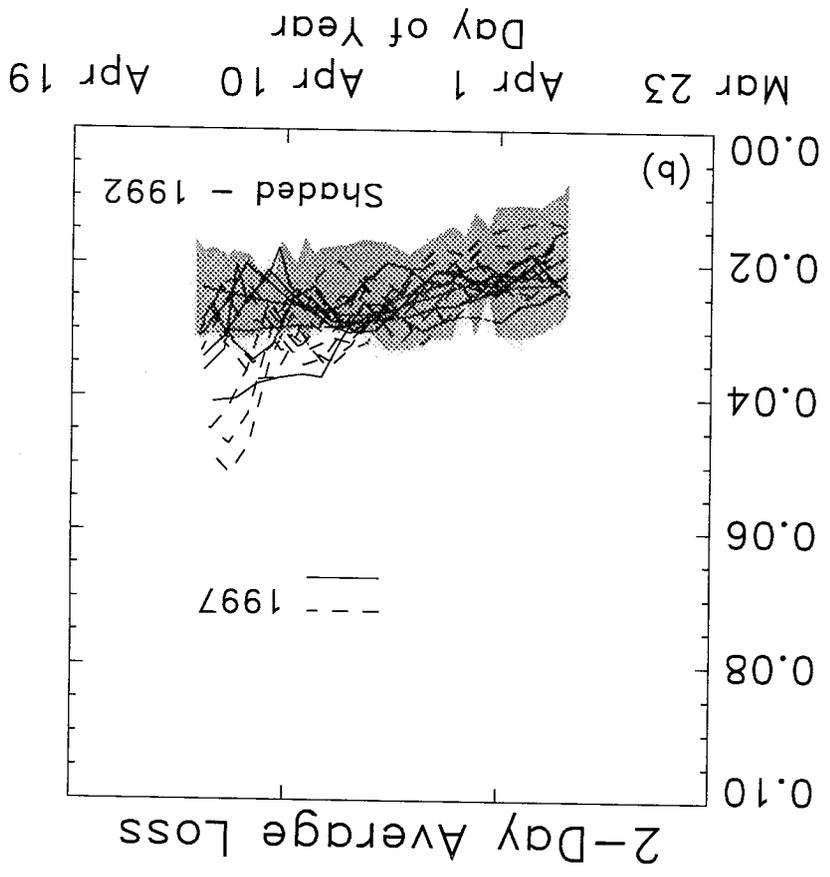Plate 1. Comparisons of model values at the location of HALOE observations at 00z on the date of the HALOE observation for NO_x (top row); O_3 (middle row); HCl (bottom row) for April 1992 (leftmost column); July 1992 (left center column; April 1997 (right center column) and June 1997 (rightmost column); all HALOE observations north of 50°N are considered.
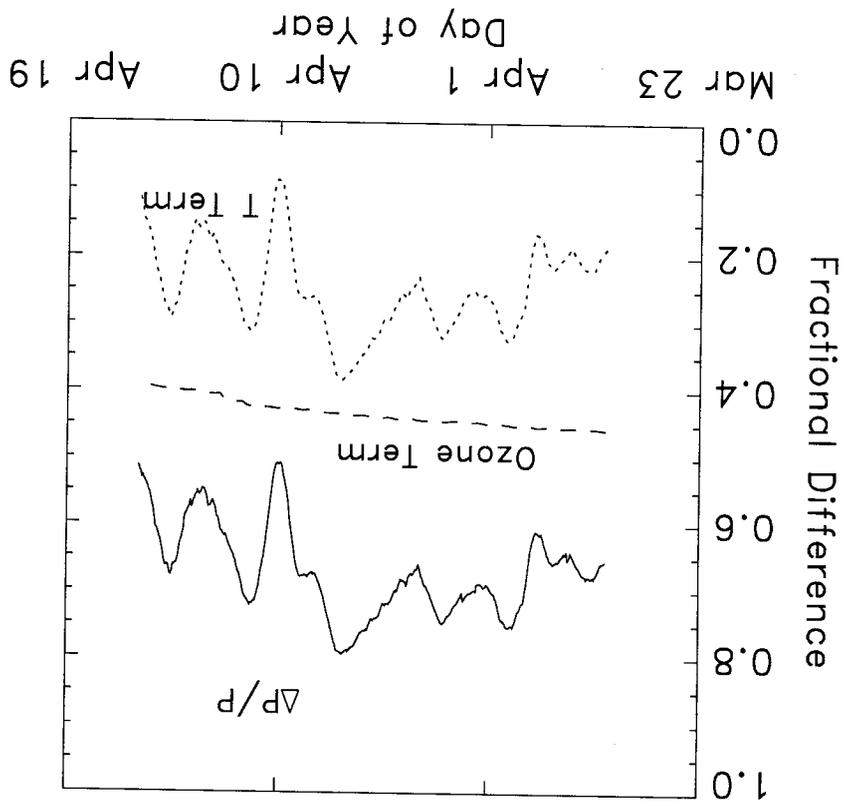
Plate 2. The May 15 1997 model O_3 on the 500 K surface (top left) and the model HCl on the 500 K surface (bottom left); filled circles locate the HALOE observations. The HALOE observations for HCl (crosses, bottom right) and the difference O_3 - zonal mean) (crosses, top right) show much of the same structure that is found in the model fields (solid lines).
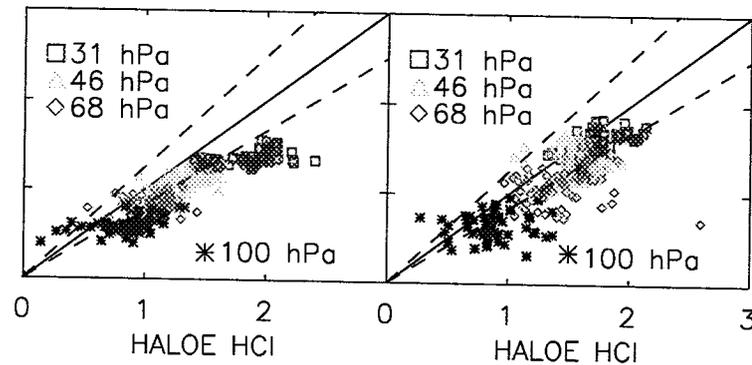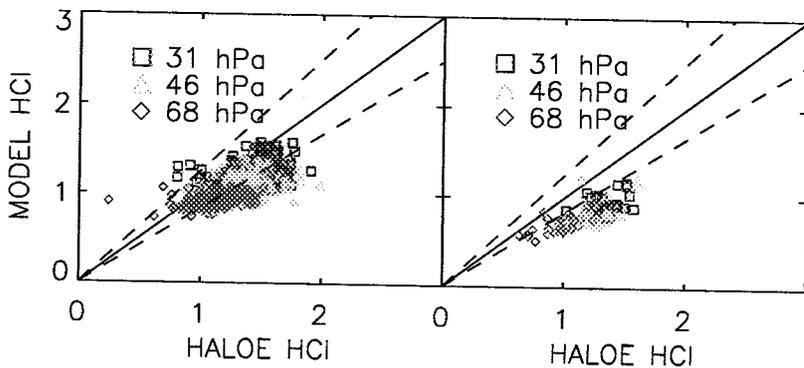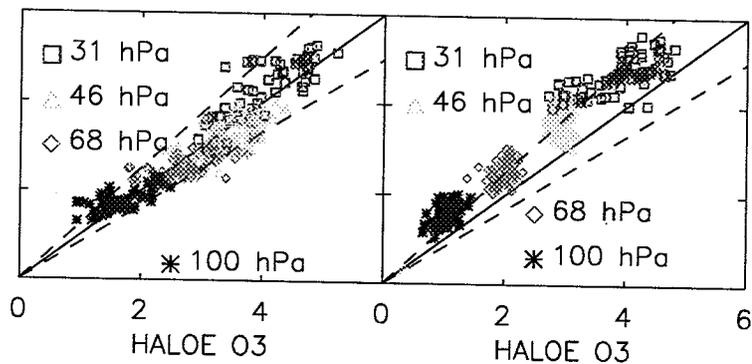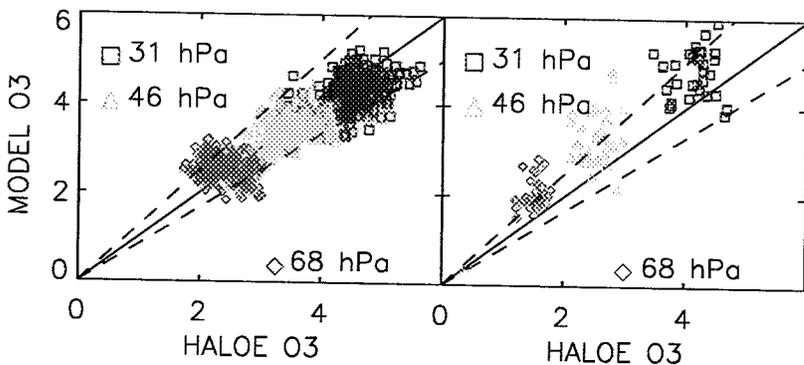
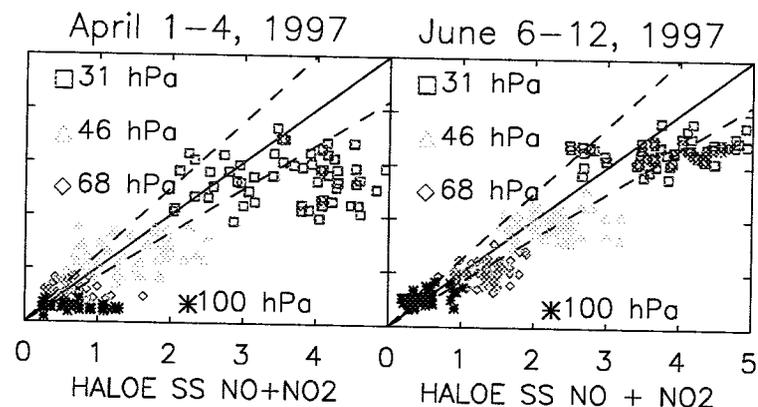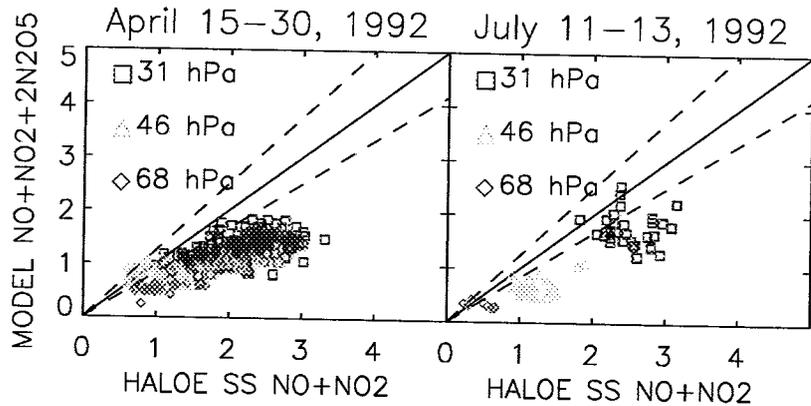Plate 3. The evolution of the fractions of Cly for HCl, ClO and $ClONO_2$ as modeled and observed by MLS (ClO), HALOE (HCl) and CLAES ($ClONO_2$) for 1992 (a) and 1997 (b).

(c)

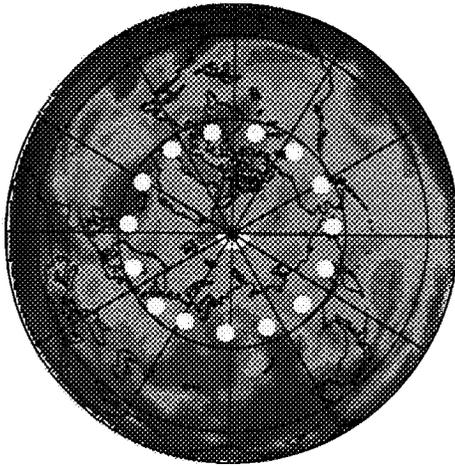3D HCl$_f$ −HCl$_i$ (ppbv)
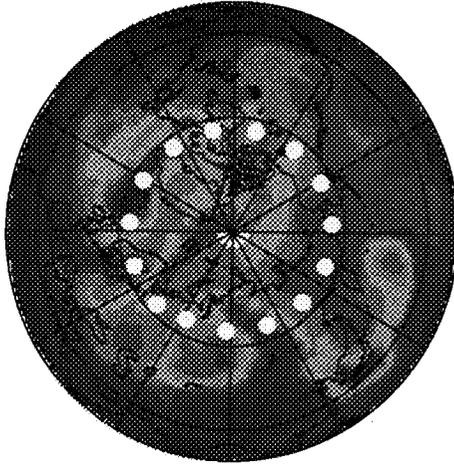
Traj HCl$_f$ −HCl$_i$ (ppbv)

◇ 1997
+ 1992

(b)

Day of Year

Mar 23   Apr 1   Apr 10   Apr 19

HCl (ppbv)

1997

(a)

HCl (ppbv)

1992

(b)

Shaded – 1992

1997

2-Day Average Loss

ppbv/day

0.00 0.02 0.04 0.06 0.08 0.10

Day of Year

Mar 23   Apr 1   Apr 10   Apr 19

(a)

Shaded – 1992

1997

2-Day Average Production

ppbv/day

0.00 0.02 0.04 0.06 0.08 0.10

Day of Year

Mar 23   Apr 1   Apr 10   Apr 19

April 15-30, 1992   July 11-13, 1992   April 1-4, 1997   June 6-12, 1997

Plate 1

500 K O3 May 15 1997

500 K HCl May 15 1997

ppmv

1.00

4.00

ppbv

0.0

2.00

O3 - mean (ppmv)

-1.0 -0.5 0.0 0.5 1.0

0

100

200

300

Longitude

O3 500 K May 15 1997

HCl - mean (ppbv)

-1.0 -0.5 0.0 0.5 1.0

0

100

200

300

Longitude

HCl 500 K May 15 1997

Plate 2

(a) 500 K 1992

(b) 500 K 1997

Plate 3